Proceedings of the 6th International Conference on Civil Engineering for Sustainable Development (ICCESD 2022), 10~12 February 2022, KUET, Khulna, Bangladesh (ISBN-978-984-35-1972-6)

NUMERICAL STUDY OF THE BEHAVIOUR OF STAINLESS STEEL SEMI-RIGID JOINTS

Swachchha Salila Saha*[1], A S M Kaysaru Zaman Kawshiq[2] and Shameem Ahmed[3]

[1] *Student, Department of Civil Engineering, Bangladesh University of Engineering and Technology, Bangladesh, e-mail: swachchhasalila37@gmail.com*
[2] *Student, Department of Civil Engineering, Bangladesh University of Engineering and Technology, Bangladesh, e-mail: kawshiqkhan@gmail.com*
[3] *Associate Professor, Bangladesh University of Engineering and Technology, Bangladesh, e-mail: shameemahmed@ce.buet.ac.bd*

***Corresponding Author**

ABSTRACT

Stainless steel is a very well-known structural material for its corrosion resistant property and is highly used in constructions of steel frames. Stainless steel has proven to have higher energy absorbing capacity, higher strain hardening property and higher ultimate stress than carbon steel. This study presents a numerical investigation of a stainless-steel semi-rigid joint under monotonic loading. Top-seat with double-web angle beam-column connection with pre-tensioned bolts were studied here as they are the most common semi-rigid joint in steel structures. Initially, the developed finite element model created using finite element analysis (FEA) software ABAQUS/CAE was verified with experimental results. Later, thirteen models were created to observe the influences of different geometric parameters on their moment-rotation characteristics of the joint. Material non-linearity and plastic hardening of the stainless-steel was taken into account. The effect of top and seat angle thickness, web angle thickness, bolt number and bolt pretension loads were studied in this article. It was found that with the increase of top-seat angles and web angles thickness, the ultimate moment capacity and initial stiffness were increased. However, the rotation at the ultimate moment decreased. Increasing the number of bolts in top-seat angles and beam flanges joint improved the moment capacity to some extent. On the other hand, bolt pretension load showed little to no influence on the moment-rotation behavior of the joint. The methodology used in this study can be further used for future works of similar nature.

Keywords: *Semi-rigid connection, stainless steel, finite element analysis, moment-rotation, monotonic loading*

1. INTRODUCTION

Uses of stainless steel are in increasing trend due to its better ductility, corrosion resistance and fire resistance properties (Cashell, 2014; Baddo, 2009; Gedge, 2008; Rossi, 2014). Apart from carbon-steel, stainless steel displays a rounded stress-strain curve with no definite yield point and shows significantly higher strain hardening. The elongation at fracture for stainless steel is between 40-60% and the ultimate-to-yield strength ratio is around 1.5-2.0. Several design codes are currently available for stainless steel such as SEI/ASCE-8-02, AS/NZS 4673 and EN, 1993-1-4 (American Society of Civil Engineers (ASCE), 2002; AS/NZS, 2001; EN, 1993-1-4, 2006). However, due to insufficient studies, all accessible codes do not offer any guidance for stainless steel joint design. They suggested following the design guidelines of carbon steel where the strain hardening benefits of stainless steel were not incorporated.

The structural response of individual members is the primary focus of research on stainless steel, whilst the reaction of joints has obtained far less consideration to date. The first numerical analysis into top-seat stainless steel joint was presented by Hasan et al. (Hasan et al., Numerical Investigation on the Semi-Rigid Behaviour of Austenitic Stainless Steel Connections, 2017; Hasan et al., Moment-rotation behaviour of top-seat angle bolted connections produced from austenitic stainless steel, 2017). Later, Elflah et al. (Elflah et al., 2018) observed the moment-rotation conduct of different types of beam-column joints by testing full-scale specimens. In their study, two top and seated cleat connections, one flush and one extended end plate connection, and two top and seated, and web cleat connections of single-sided beam-to-column joints were tested under static monotonic loading. Comparing these test results with the codified stipulations of EN1993-1-8 (EN, 1993-1-8, 2005), they found that the joints displayed outstanding ductility and reached loads much better than the ones expected by design standards for carbon steel connections. Hasan et al. (Hasan et al., 2019) also tested one top-seat with double web angle beam-column joint and found similar results. For proper understanding of the functioning of stainless-steel beam-column connections and formulating a design guideline, further research is needed.

The objective of the study is to observe the behavior of a stainless-steel beam-column top-seat with a double web angle semi-rigid connection under monotonic loading. For this, initially, a finite element (FE) model was established which was validated with experimental results. Later, the verified FE simulation was used in parametric study. In the parametric study the effects of the thickness of top-seat angles and web angles, and the number of bolts on the moment-rotation performance of the joint were examined. The effect of bolt pretension load on the performance of the semi-rigid joints was also observed.

2. FINITE ELEMENT MODELLING

The model of the beam-to-column joint was analyzed using commercial finite element software ABAQUS/CAE (ABAQUS, 2014). Initially, the beam-column joint tested by Hasan et al. (Hasan et al., 2019) was modeled for verification. In the model, a column of I-354×173×8×12 mm section was connected to a beam of I-328×312×16×25 mm section with 150×100×12 mm top and seat angles and 100×100×10mm web angles. Metric standard M20 grade bolts were used in the joint as shown in Figure 1. All the dimensions of the joint were taken from the experiment (Hasan et al., 2019) where the height of the column was 600 mm and the length of the beam was 1200 mm. All the elements of the joint such as column, beam, angles and bolts were modeled using incompatible 8-noded brick elements (C3D8I). The mesh size of the model varied from 2.2 mm to 50 mm. All the angles, bolts, and parts of the column and beam adjacent to the joint had finer mesh where large deformation and distortion of elements were expected. In Figure 2 the mesh distribution of the joint is presented. For simplicity, the nuts and bolt heads were modelled as round-shaped instead of hexagonal shaped.

Table 1: Material Properties (Hasan et al., 2019)

Connection Element	t or d[a] (mm)	E (MPa)	$\sigma_{0.2}$ (MPa)	σ_u (MPa)
Beam, Column	5.76	199505	335	586
Top-seat angle	5.75	201338	326	602
Web angle	4.63	191535	278	566
Bolt [a]	4.9	195380	470	639

[a] defined the diameter of the bolt element

The material properties of beam, column, angle plates, and bolts were incorporated from the experiment (Hasan et al., 2019) and tabulated in Table 1. The stress-strain behaviour of stainless steel was determined using modified Rasmussen's model (Arrayago et al., 2015). The load was applied at 75 mm from the tip of the beam to achieve a similar rotation in the connection as in the experiment conducted. Pretension load on bolts was assigned to a predefined field. Considering fixed support conditions, all degrees of freedom were restrained at the top and bottom nodes of the column. Contact behavior was assigned between all elements that came into contact with each other, such as beam end surface to column flange, beam to angles, bolts to beam and angles to column. Here, for bolt shank & the holes of the parts connected to it, friction coefficient is taken as 0.3 for tangential behavior of the contact surface

& small sliding was allowed. Rest of the contact surfaces were set as frictionless, finite sliding was allowed. The normal behavior of the contact was defined as "hard-contact" where no penetration was allowed. However, all surfaces were allowed to get separated after contact.

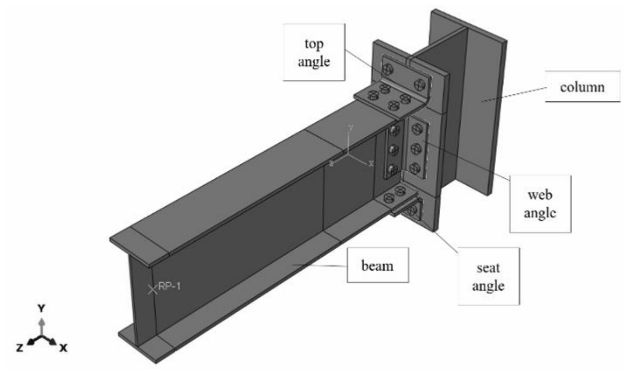

Figure 1: Details of joint

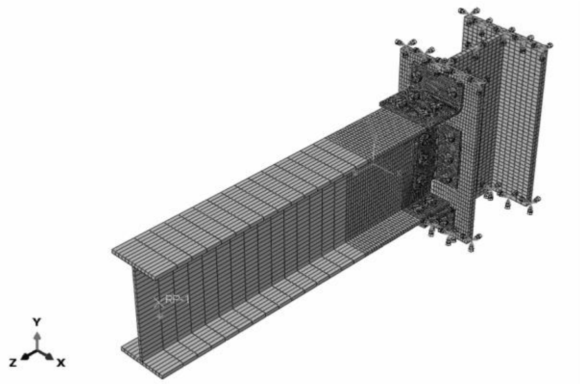

Figure 2: Loading and support condition on the meshed model

3. VERIFICATION OF FE MODEL

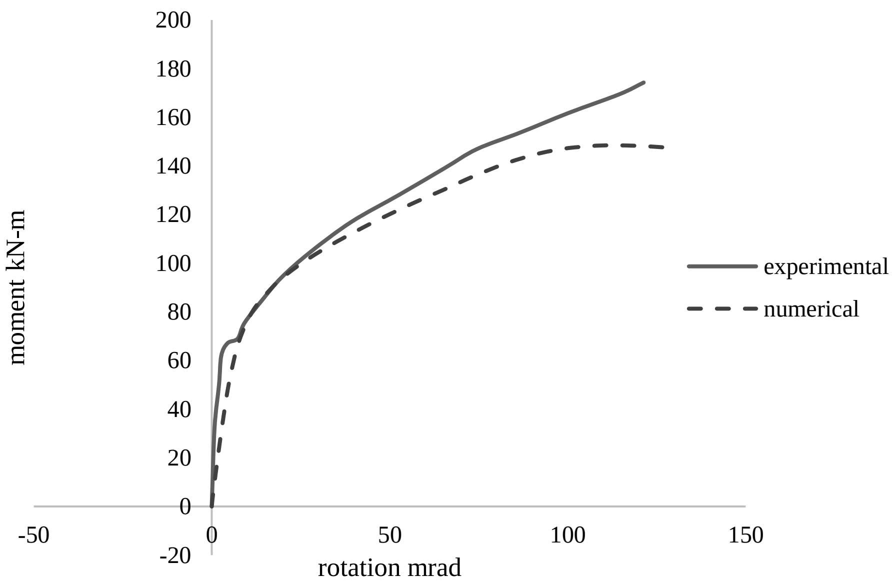

Figure 3: Verification of Moment-Rotation Curve between Experimental and FE model

The functioning of the finite element model developed here was evaluated by comparing the results of the FE analysis with the experiment results of Hasan et al. (Hasan et al., 2019). Both moment-rotation behaviour and deformation shapes were considered here. The moment at the column face versus rotation angle from FE analysis and experimental investigation is presented in Figure 3. It is detected that the FE analysis and experimental outcomes are very similar up to 90 mrad rotation. After that, the numerical results showed slightly less moment capacity than the experiment. The variation in rotation is only 1.25%. Figure 4 (a), (b), (c), (d), (e), and (f) illustrate the deflected shapes of the joint and its different elements obtained from experiment and FE analysis. The deflected shapes show that they are identical in nature. In the comparison, it is clear that the FE model is able to simulate the behaviour of beam-column joints with good accuracy. Therefore, this model can be treated to study the behaviour of semi-rigid beam-column joints.

(a) Deformation of connection just after the test (Hasan et al., 2019)

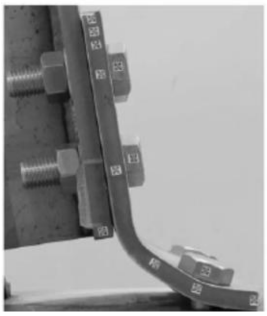

(c) Deformation of top angle after test (Hasan et al., 2019)

(e) Deformation of bolt after test (Hasan et al., 2019)

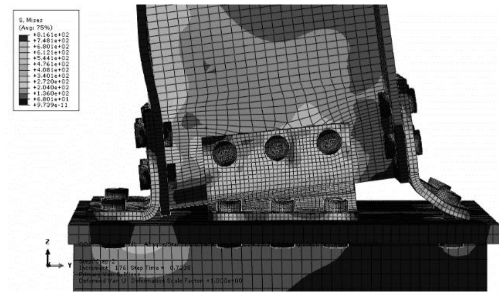

(b) Deformation of connection attained from FEA at the end

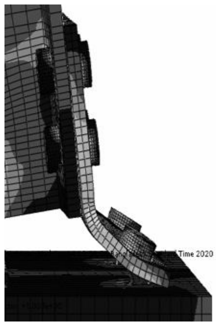

(d) Deformation of top angle from FEA

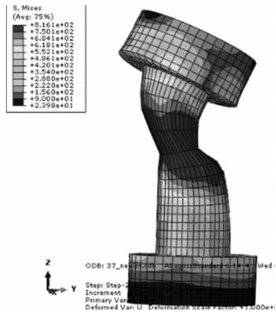

(f) Deformation of bolt from FEA

Figure 4: Comparison of deformed shape of parts of Experimental and FE analysis

4. PARAMETRIC STUDY

A parametric study was organized in this section to better understand the behavior of the stainless steel semi-rigid joint. In the parametric study, the thickness of top and seat angles, the thickness of the web angles, the number of bolts between top-seat angles and beam, and the number of bolts between column and top-seat angles were varied. The variable dimensions of different models are presented in Table 2. All other dimensions were taken to be the same as the dimensions of the verified model. A total of nine models were analyzed for incorporating geometric variation where the BASE model was the model used in verification. The other five models were also analyzed to observe the effect of bolt pretension load.

Table 2: Different Parameters

Specimen	Thickness [mm]		Number of Bolts			
	Top-Seat Angle	Web Angle	Top-Seat Angle		Web Angle	
			Beam	Column	Beam	Column
BASE	12	10	4	2	3	3
TST 1	16	10	4	2	3	3
TST 2	8	10	4	2	3	3
WAT 1	12	No-web angle	4	2	-	-
WAT 2	12	6	4	2	3	3
WAT 3	12	14	4	2	3	3
BSB 1	12	10	2	2	3	3
BSB 2	12	10	6	2	3	3
CSB 1	12	10	4	4	3	3

4.1 Effect of the Thickness of Top-Seat Angle

The impact of the thickness the of top and seat angles on the moment-rotation behavior of the joint is presented here. In this study, the thickness of top-seat angles varied from 8mm to 16 mm. The moment rotation behavior of the joints with different top-seat angle thicknesses is presented in Figure 5. Figure 6 and 7 present the variation of ultimate moment and rotation at the ultimate model with the angle thickness respectively. From the figures, it is observed that with the increase of top-seat angle thickness the ultimate moment capacity and initial stiffness of the joint increased, and the rotation at the ultimate moment decreased.

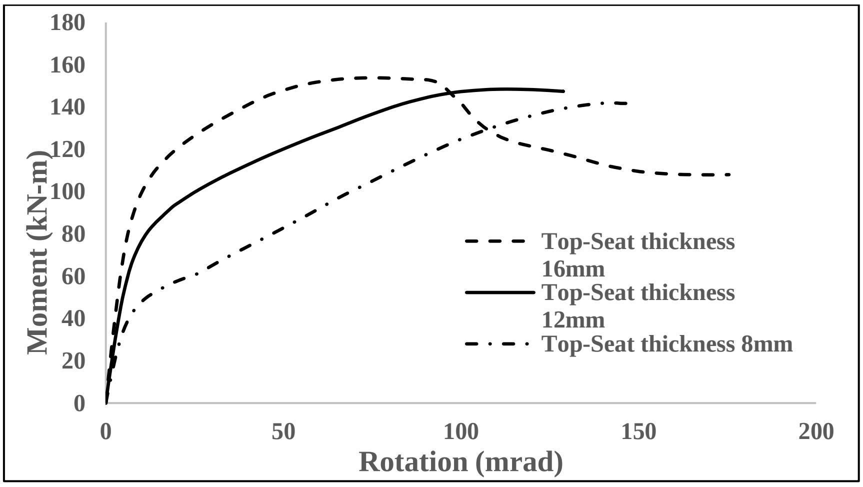

Figure 5: Moment-Rotation curve for top-seat angle thickness analysis

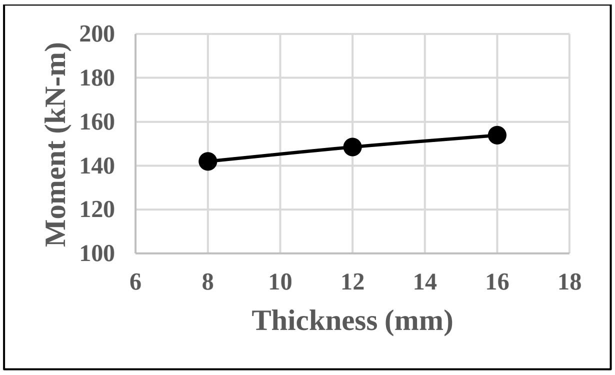

Figure 6: Moment-Thickness curve for top-seat angle thickness analysis

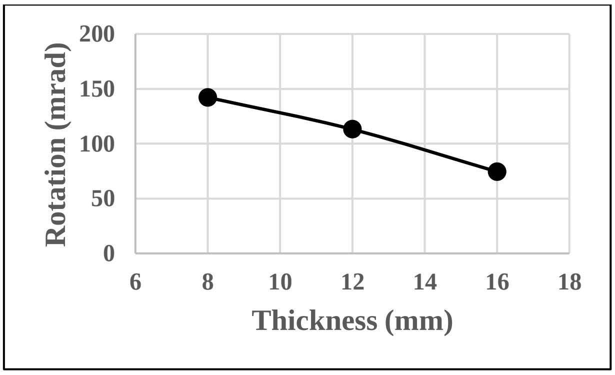

Figure 7: Rotation-Thickness curve for top-seat angle thickness analysis

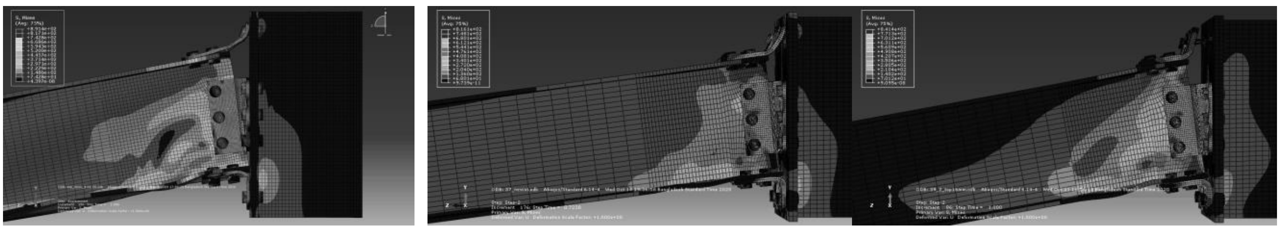

(a) Top-Seat thickness 8mm (b) Top-Seat thickness 12mm (c) Top-Seat thickness 16mm

Figure 8: Deformed Shape of the Joint (Top-Seat angle thickness analysis)

From Figure 6, it is found that with an increase in thickness from 8 mm to 16 mm the ultimate moment capacity improved by 8%. However, the decrease in rotation is more prominent with the increase of top-seat angle thickness. The rotation at the ultimate moment decreases from 142 mrad to 74 mrad with the increase of thickness from 8 mm to 16 mm. In Figure 8, the deflected shapes of the models with different top-seat angle thicknesses are shown.

4.2 Effect of Double Web Angle

The impact of web angle thickness was observed by altering the thickness from 6 mm to 14 mm. A model without any web angle was also analyzed. Moment vs rotation curves of the joints without web angle and with different thicknesses of web angles are presented in Figure 9. Figure 10 and 11 present the variation of moment and rotation at the ultimate moment for different web angle thicknesses and without web angle. Figure 10 and 11 show that by adding a web angle of 6 mm the ultimate moment capacity increased by 22.15% and rotation at the ultimate moment increased by 21.02%. When the thickness of web angles increased from 6 mm to 10 mm, ultimate moment resisting capacity also saw an increase of 32.33% and corresponding rotation decreased by 3.53% Again, with a further increase in thickness from 10 mm to 14 mm the ultimate moment also increased by 6.30% with a reduction of 13.60% in rotation. The initial stiffness of the joints was also increased with the increase in web angle thickness. In Figure. 12, the deflected shapes of the models with different web angle thicknesses are shown.

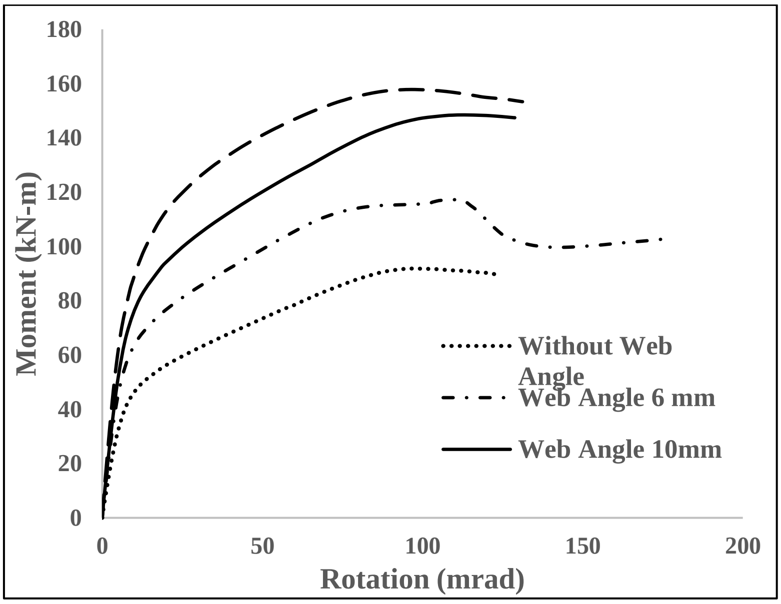

Figure 9: Moment vs Rotation Curve for Web Angle thickness analysis

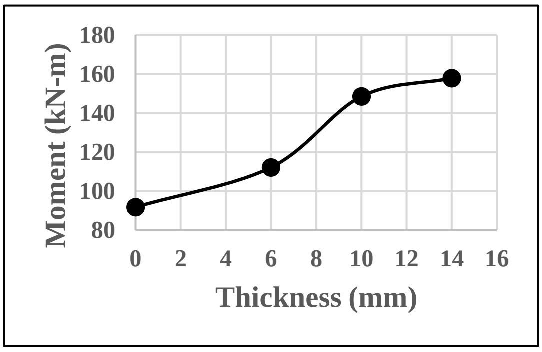

Figure 10: Moment-Thickness curve for Web angle thickness analysis

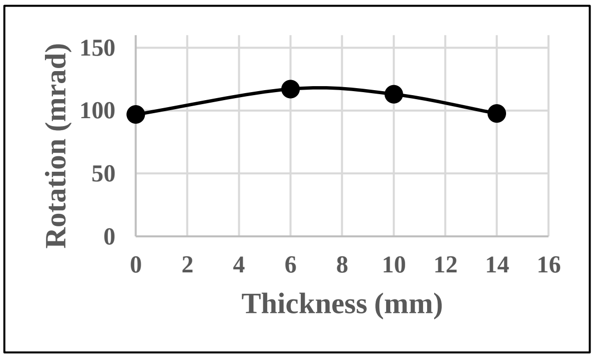

Figure 11: Rotation-Thickness curve for Web angle thickness analysis

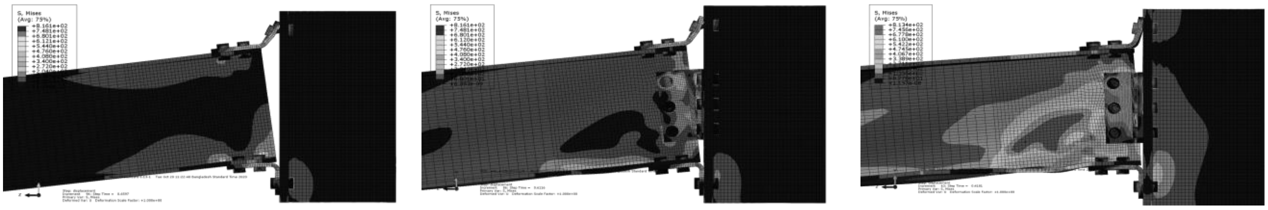

(a) Without Web-angle (b) Web angle thickness 6 mm (c) Web angle thickness 14 mm

Figure 12: Deformed Shape of the Joints (Web-Angle thickness analysis)

4.3 Effect of Number of Bolts in Beam

For finding the effect of the number of bolts in the top-seat connecting to the beam flange, three specimens BASE, BSB 1, BSB 2 were analyzed. They had 4 bolts (in 2 rows), 2 bolts (in 1 row), and 6 bolts (in 3rows) in the top-seat angle connecting to the beam flange respectively. With a change in the number of rows of bolts, the length of the top-seat angle also changed. All other parameters like the diameter and spacing of bolts were unchanged. The effect of varying bolt numbers on moment-rotation curves is shown in Figure 13.

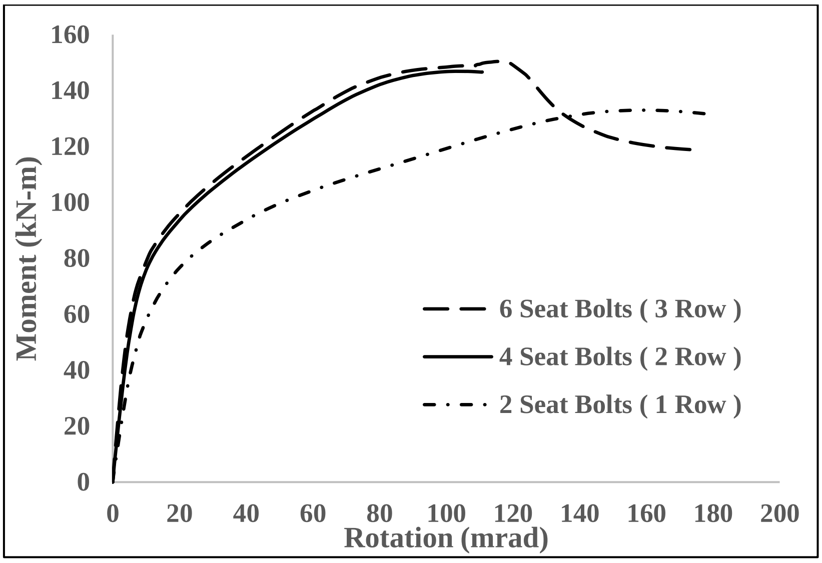

Figure 13: Moment vs Rotation Curve for Top-Seat Bolts in Beam Flange Analysis

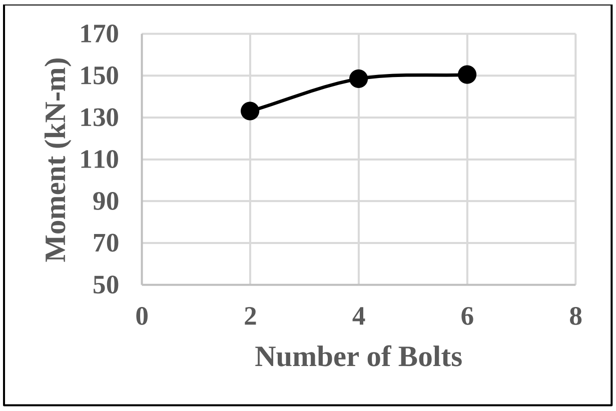

Figure 14: Moment vs Number of Seat Bolts in Beam curve

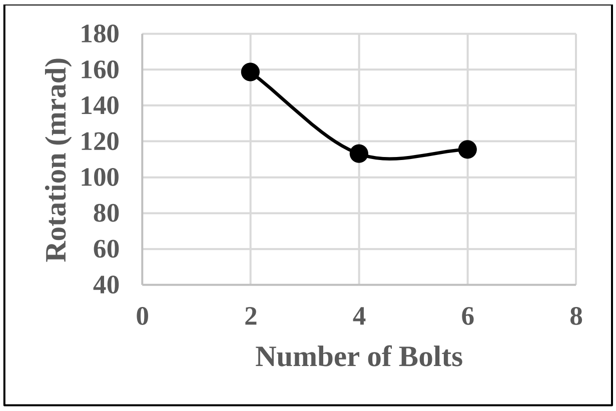

Figure 15: Rotation vs Number of Seat Bolts in Beam curve

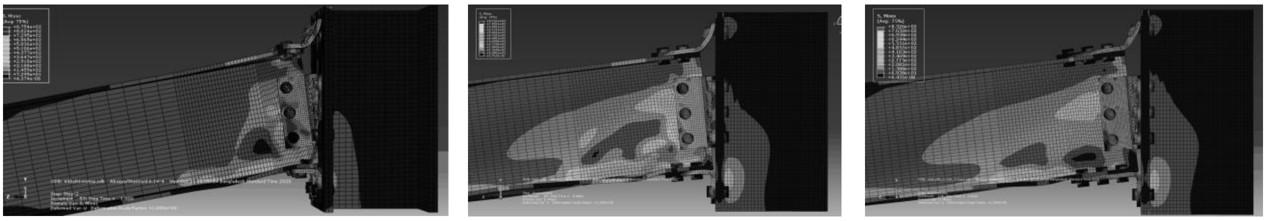

(a) 2 Number of bolts (1 Row Top-Seat Bolts)   (b) 4 Number of bolts (2 Row Top-Seat Bolts)   (c) 6 Number of bolts (3 Row Top-Seat Bolts)

Figure 16: Deformed Shape of the Joints (Top-Seat Bolts in Beam Flange Analysis)

Also, from Figure 14 and 15, it was seen that with the increase in number of bolts, moment capacity increased and rotation was decreased. When the number of bolts increased from 2 to 4, moment capacity increased by 10% and rotation decreased by 40%. On the other hand, by increasing the number of bolts from 4 to 6, the change in ultimate moment and rotation is insignificant. In Figure 16, the deflected shapes of the models with different numbers of bolts are presented.

4.4 Effect of Number of Bolts in Column

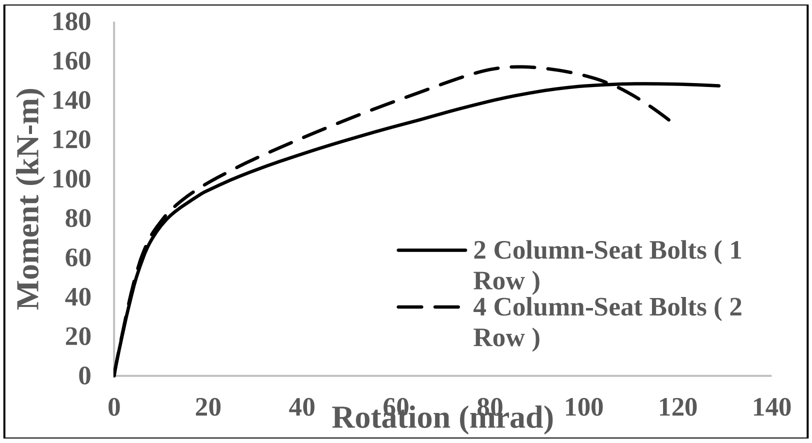

Figure 17: Moment vs Rotation Curve for Top-Seat Bolts in Column Flange Analysis

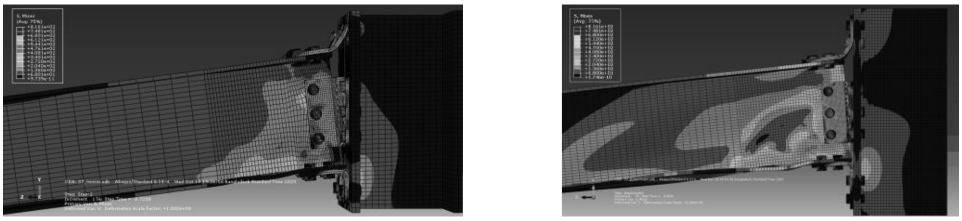

(a) 2 Number of bolts (1 Row Top-Seat Bolts)   (b) 4 Number of bolts (2 Row Top-Seat Bolts)

Figure 18: Deformed Shape of the Joint (Top-Seat Bolts in Column Flange Analysis)

The impact of the number of bolts between top-seat angles and column flange was analyzed by two models BASE and CSB 1, where the number of bolts was changed from 2 to 4 respectively. Due to the change in the number of bolts and rows, the length of top-seat angle on the column flange also increased but every other parameter was kept unchanged. From moment vs rotation curves, as illustrated in Figure 17, it is observed that with an increased number of bolts moment capacity increased, and at the same time, rotation decreased. By increasing the number of bolts from 2 to 4, the ultimate moment increased by 5.78% and rotation decreased by 23.50%. In Figure 18, the deflected shapes of the models with different numbers of bolts are presented.

4.5 Effect of Bolt Pre-Load

To assess the effect of bolt pretension load, the BASE model was analyzed by applying different pretension loads. The bolt pretension load varied from 20% to 60% of their proof load. The results of the investigation are shown in Table 3. It is observed that all the bolt preloads produce a very similar result with no significant difference.

Table 3: Results of the models with different Bolt Pretension Loads

Specimen	Bolt Pre-Loads [N/mm^2]	Ultimate Moment [kN-m]	Rotation at Ultimate moment [mrad]
20% Pre-Load	100	148.46	113.072
30% Pre-Load	150	148.52	114.900
40% Pre-Load	200	146.91	108.089
50% Pre-Load	250	147.60	101.982
60% Pre-Load	300	147.61	101.987

5. CONCLUSIONS

In this paper, the performance of a stainless-steel beam-to-column top-seat with a double web angle semi-rigid connection under monotonic loading was studied. Using a verified FE model, the moment rotation behavior of the joint was observed for different thicknesses of top-seat and web angles. The effect of bolt numbers and bolt pretension load were also examined. It was found that with the increase of top-seat angle thickness, the ultimate moment capacity and preliminary stiffness of the joint increased. However, the rotation at the ultimate moment decreased. Changing the thickness of the double-web angles also had a similar effect on the joint. With the increase in the number of bolts between top-seat angles and beam flanges, initially, the ultimate moment capacity and initial stiffness increased. Increasing the number of bolts beyond 2 rows will not improve the moment capacity of the joint. Increasing the number of bolts from one row to two rows between the top-seat angles and the column flange had no significant impact on the ultimate moment capacity and initial stiffness of the joint. Increasing the bolt pre-load from 20% to 60% of the bolt pre-load had virtually no effect on the joint.

ACKNOWLEDGEMENTS

The authors express their profound gratitude towards Almighty for giving them the opportunity to complete this research work. We sincerely thank our respected supervisor Dr. Shameem Ahmed without whom this work would not be possible. We are grateful to all who were supporting us on our journey.

REFERENCES

American Society of Civil Engineers (ASCE), (2002). *Specification for the design of cold-formed stainless steel structural members, SEI/ASCE-8-02.* Virginia, USA: ASCE Standard.

Arrayagoa, I., Reala, E. and Gardner, L. (2015). Description of stress-strain curves for stainless steel alloys, *Materials and Design 87*, 540-552, August.

AS/NZS, (2001). *Australian/New Zealand Standard (AS/NZS), in Cold-formed stainless steel structures 4673*. Sydney, Australia: Standards Australia.

Baddo, N.R. (2008). Stainless steel in construction: a review of research, applications, challenges and opportunities. *J. Constr. Steel Res. 64 (11)* 1199–1206.

Baddo, N. R. and Cashell, K. A. (2014). Ferritic Stainless Steel in Structural Application., *Thin-Walled Struct.83,* 169-181.

Dassault Systemes Simulia Corp. (2014). ABAQUS. ABAQUS/CAE User's Manual v6.14: Elements, Providence, RI, USA.

Elflah, M., Theofanous, M., Dirar, S. and Yuan, H. (2018). Behaviour of stainless steel beam-to-column joints — part 1: Experimental investigation. *Journal of Constructional Steel Research, 11.*

EN, 1993-1-4. (2006). Eurocode 3: *Design of Steel Structures - Part 1–4, in General Rules - Supplementary Rules for Stainless Steels*. Brussels: European Committee for Standardization.

EN, 1993-1-8. (2005). Eurocode 3: *Design of Steel Structures – Part 1-8: Design of Joints*. British Standards Institution, CEN.

Gedge, G. (2008). Structural uses of stainless steel — buildings and civil engineering. *Journal of Constructional Steel Research*, 1194–1198.

Hasan, M. J., Al-Deen, S. and Ashraf, M. (2019) Behavior of top-seat double web angle connection produced from austenitic stainless steel. *Journal of Constructional Steel Research 155,* 460-479.

Hasan, M. J., Ashraf, M. and Uy, B. (2017). Numerical Investigation on the Semi-Rigid Behaviour of Austenitic Stainless Steel Connections, *Ce/Papers 1(2–3),* Copenhagen, Denmark, September 13-15, 215–224.

Hasan, M. J., Ashraf, M. and Uy, B. (2017). Moment-rotation behaviour of top-seat angle bolted connections produced from austenitic stainless steel. *Journal of Constructional Steel Research (136), Supplement C.,* 149–161.

Rossi, B. (2014). Discussion on the use of stainless steel in constructions in view of sustainability., *Thin-Walled Struct. 83,* 182–189.